

# The Effect of Field Damping on Rotordynamics of Non-salient Pole Generators

F. Boy, H. Hetzler

*This paper investigates the influence of magnetic field damping on lateral shaft oscillations of non-salient pole generators. Field damping is caused by compensating currents affecting the magnitude and orientation of the magnetic field and resulting lateral forces. These currents can either occur in especially constructed devices, like a damper cage, or simply in the core material as eddy currents. While damper windings are used to reduce torsional shaft vibrations by generating an asynchronous damper torque, this survey reveals that in contrary to intuition, the field damping in general may cause self-excited lateral shaft oscillations leading to noise emission and reliability issues. It is shown that the effect is strongly dependent upon the machine type and the nominal rotational speed compared to the critical speed. The applied approach is analytical taking into account arbitrary lateral rotor motion in the context of linear rotordynamics.*

## 1 Introduction

The main purpose of an electric generator is the conversion of mechanical to electrical power. To do so an electromechanical torque is transmitted by a rotating magnetic field which originates from currents flowing in the stator and rotor windings and from compensating currents in damper windings or the core material, respectively. However, the magnetic field also causes reluctance stresses at the air gap surface. Especially when the rotor runs eccentrically in the stator bore, these stresses are unbalanced, causing unbalanced magnetic forces. The most important one, pointing towards the direction of the smallest air gap is denoted as unbalanced magnetic pull (UMP) and has been studied extensively in the past century, as summarised for example by Kaehne (1963). However, in view of rotordynamics and the evolution of lateral shaft oscillations, especially the force component perpendicular to the UMP plays an important role due to the fact that it can feed and remove comparably large amounts of energy to and from the orbital motion of the rotor. Effects influencing the perpendicular force component have been investigated mainly in asynchronous machines due to the fact that squirrel cage rotors cause strong perpendicular forces (Früchtenicht, 1982). Furthermore, there are a lot of additional influences changing the amplitude and direction of the magnetic force. Among them are effects due to parallel paths in the windings, as investigated by Burakov (2006), magnetic homopolar fluxes (Belmans, 1987) and saturation (Arkkio, 2000).

Damper windings are another interesting example affecting the force. Usually, their purpose is to reduce torsional shaft vibrations (Jordan, 1970). However, as shown by Dorell et al. (2011) for asynchronous machines and by Wallin et al. (2013) for salient pole generators, damper windings may also change the direction of the lateral electromagnetic forces.

This study discusses the influence of field damping on the rotordynamics of non-salient pole generators as a similar question to the studies mentioned above. The machines being considered here, usually run at higher speeds, making effects due to dynamic rotor eccentricity more relevant. While only some of them actually possess damper windings, field damping as a general qualitative phenomenon, might also be caused by eddy currents in the rotor core material resulting in an analogous effects.

This study extends existing surveys by Kellenberger (1966) and the authors (Boy, 2016), which found that the forces and thus the rotordynamics of turbogenerators are strongly dependent on the load condition. In the present work, it is shown, that field damping might cause self-excited lateral shaft oscillations at higher rotational speeds. Their dependency on the machine design, occurring homopolar flux and load condition will be outlined.

The applied modelling approach is an analytical one. Solving the combined electro-mechanical problem by space vector theory and assuming stationary speed of operation, the forces of electromagnetic origin are derived for an arbitrary orbital motion of the rotor. With this information a stability analysis of the steady state, indicating the occurrence of self-excited oscillations is carried out. All symbols introduced subsequently are explained in the text.

Additionally a nomenclature is given in the appendix.

## 2 Model

Investigating electrical machine rotordynamics involves the solution of three subproblems (Fig. 1): The current flowing in the electrical circuits are sources to the magnetic field in the air gap of the machine. The changing magnetic flux in return induces voltage into these circuits. Furthermore the magnetic field exerts forces on the rotor of the machine, while the rotor motion in return distorts the air gap domain and thus affects the magnetic field.

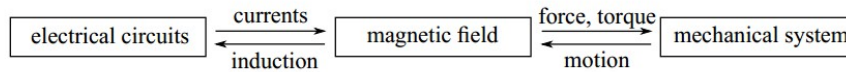


Figure 1. Electro-mechanical machine model involving three subproblems.

### 2.1 Assumptions and Kinematics

To analytically solve the magnetic field problem several assumptions have to be made. Both stator and rotor shall be perfectly aligned cylinders (radii  $r_1$  (stator) and  $r_2$  (rotor)). The material shall be infinitely permeable, allowing to restrict the consideration to the air gap domain but excluding saturation effects. The problem shall be two-dimensional, neglecting axial boundary effects and corresponding stray losses. The actual windings in the slots are replaced by current sheets  $a_1$  and  $a_2$  for the stator (index 1) and the rotor (index 2) respectively. This simplification is permissible according to the field equivalence principle for sufficiently smooth surfaces, as it is the case in non-salient pole machines. The involved compensating currents shall be represented by currents in damper windings (index D), realised comparable to the squirrel cage of an induction machine with  $N_D$  bars, which are continuously connected by conducting rings at the axial ends of the rotor. Corrections in the air gap width due to slotting or in the winding factors due to skewed damper bars etc. are left out here, as the study is concerned with qualitative effects.

Fig. 2 shows an overview of the field domain and the involved kinematics. For the description of the problem several frames of reference are introduced: A cartesian inertial frame of reference  $\mathcal{K}_1 = [O, \{\vec{e}_{x_1}, \vec{e}_{y_1}, \vec{e}_{z_1}\}]$ , one where the  $x$ -axis is pointing towards the direction of eccentricity (smallest air gap), denoted as  $\mathcal{K} = [O, \{\vec{e}_x, \vec{e}_y, \vec{e}_z\}]$  and one, identified by  $\mathcal{K}_2 = [O, \{\vec{e}_{x_2}, \vec{e}_{y_2}, \vec{e}_{z_2}\}]$ , where the  $x$ -axis shall be aligned with a distinct pole axis of the rotor. Analogous to these coordinate systems, cylindrical systems  $\mathcal{Z}_1, \mathcal{Z}$  and  $\mathcal{Z}_2$  are defined. The magnetic field problem in the air gap  $\Omega$  will be stated in cylindrical coordinates, with the radial coordinate  $r$  and corresponding angles  $\theta_1 = \theta + \gamma = \theta_2 + \vartheta$ .

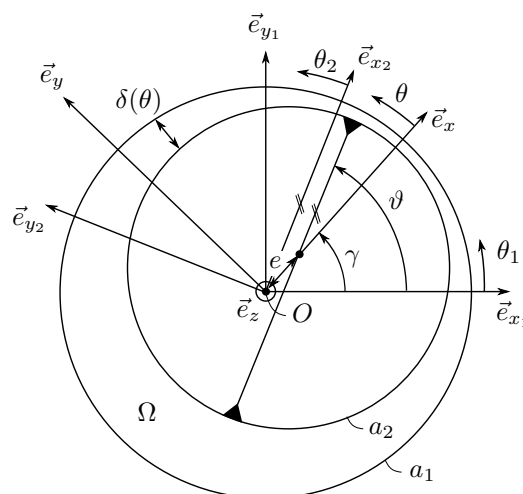


Figure 2. Kinematics and field domain.

The rotor position can either be described by polar  $(e, \gamma)$ , or cartesian coordinates  $(x_1, y_1)$ ,  $(x, y)$  and  $(x_2, y_2)$  in the different frames of reference. The absolute angular orientation of the rotor is described by the angle  $\vartheta$ . Note that all angles  $\theta_i$  (with some index  $i$ ) represent spatial coordinates, while  $\gamma$  and  $\vartheta$  are discrete mechanical coordinates. Later on, different electrical angles  $\varphi_k$  will be introduced. They transform with  $\varphi_k = p\vartheta_k$  to a corresponding mechanical angle  $\vartheta_k$ .

With the kinematic definitions and physical simplifications stated before and assuming that the mean air gap width  $\delta_m = r_1 - r_2$  is small compared to the rotor radius  $\left(\varepsilon = \frac{\delta_m}{r_2} \ll 1\right)$ , it can be shown that the magnetic field of order  $\mathcal{O}(1)$  is orientated straight radially neglecting terms of higher order  $\mathcal{O}(\varepsilon)$ .

Due to circumferential periodicity the one dimensional magnetic flux density can be written as a Fourier series

$$B = B_0 + \sum_{\nu=1}^{\infty} \underbrace{\hat{B}_{\nu} \cos(\nu\theta_2 - \varphi_{B\nu})}_{B_{\nu}} = B_0 + \sum_{\nu=1}^{\infty} \text{Re} \left\{ \underline{B}_{\nu} e^{-j\nu\theta_2} \right\}, \quad (1)$$

here expressed in the frame of reference  $\mathcal{Z}_2$ , corotating with the rotor. In this equation each harmonic resembles a rotating field wave of different circumferential velocity. In eq. (1) complex notation was introduced, where  $j$  is the imaginary unit and  $\underline{B}_{\nu} = \hat{B}_{\nu} e^{j\varphi_{B\nu}}$  represents the complex amplitude of the  $\nu$ -th field harmonic. Here and further on underlining shall indicate complex variables  $\underline{A}$  and overlining their complex conjugate  $\overline{A}$ . In the context of this work only the fundamental wave of order  $p$  (where  $p$  is the number of pole pairs) and the eccentricity waves of order  $p \pm 1$  are regarded. This assumption is justified in machines with a sufficiently well arranged winding design.

Deriving an approximate solution to the magnetic field (which means finding  $B_0, \hat{B}_p, \hat{B}_{p \pm 1}$  and  $\varphi_{Bp}, \varphi_{Bp \pm 1}$ ) presumes solving of the voltage equations of the equivalent electrical circuits. These circuits are a representative phase of the stator and a representative mesh of the damper cage. To derive the induced voltages, it has to be considered that the field waves of order  $\nu$  induces alternating voltages of different frequency in the stator windings (index 1) and damper cage (index D) respectively. Thus, the voltage in an equivalent circuit (see e.g. Jordan (1970)) can be written as

$$u_i(t) = \sum_{\nu=1}^{\infty} \hat{u}_{i\nu} \cos(\omega_{i\nu}t + \varphi_{i\nu}) = \sum_{\nu=1}^{\infty} \text{Re} \left\{ \sqrt{2} \underline{U}_{i\nu} e^{j\omega_{i\nu}t} \right\} \quad (2)$$

where  $i = (1, D)$  is an index and  $\underline{U}_{i\nu} = \frac{\sqrt{2}}{2} \hat{u}_{i\nu} e^{j\varphi_{i\nu}}$  is the complex phasors of the  $\nu$ -th voltage harmonic. The frequencies are related by  $\omega_{D\nu} = s_{\nu}\omega_{1\nu}$ . In synchronous operation the slip is  $s_p = s = 0$  and the higher field harmonic slips become  $s_{p \pm 1} = 1 - \frac{p \pm 1}{p}(1 - s) = \mp \frac{1}{p}$ .

As the currents in the mentioned circuits are caused by these voltages, they can be expressed similarly. Each order of these AC quantities can be treated separately balancing only the complex phasors, which will be done subsequently.

## 2.2 Fundamental Field Harmonics

The voltage equations of order  $p$  are

$$\underline{U}_{1p} = (R_{1p} + j\omega L_{1p}) \underline{I}_{1p} + \underline{U}_{12p} \quad (\text{stator}), \quad (3)$$

$$0 = (R_{Dp} + js\omega L_{Dp}) \underline{I}_{Dp} \Rightarrow \underline{I}_{Dp} = 0, \quad (\text{damper cage}). \quad (4)$$

Here  $\underline{U}_{1p} = U_{1p}$  is the phasor of the supply voltage, which shall be aligned with the real axis without loss of generality. The phasor of the synchronous generated voltage in eq. (3) is  $\underline{U}_{12p} = U_{12p} e^{j\varphi_{12p}}$ , with the effective value  $U_{12p}$  and the polar wheel angle  $\varphi_{12p}$ . Note that there is no mutual induction of order  $p$  between the rotating field and the damper cage, as they are assumed to move synchronously ( $s = 0$ ).

Inserting  $\underline{U}_{12p}$  into eq. (3), neglecting the resistive component (as usual for larger machines (Jordan, 1970)) and solving for  $\underline{I}_{1p}$  yields

$$\underline{I}_{1p} = -j \frac{U_{1p}}{\omega L_{1p}} + j \frac{U_{12p}}{\omega L_{1p}} e^{j\varphi_{12p}}. \quad (5)$$

The fundamental field harmonic is

$$B_p = \frac{\mu_0}{\delta_m} \text{Re} \left\{ k_{1p} \underline{I}_{1p} e^{j(\omega t - p\theta_1)} + k_{2p} i_2 e^{-jp\theta_2} \right\}, \quad (6)$$

where  $\mu_0$  is the magnetic constant,  $k_{1p}$  and  $k_{2p}$  are constants depending on the machine geometry and winding design and  $i_2$  is the DC excitation current. Transforming to corotating coordinates  $\mathcal{Z}_2$  using  $\theta_1 = \theta_2 + \vartheta$ , with  $p\vartheta = \omega t - \frac{\pi}{2} + \varphi_{12p}$ , inserting  $\underline{I}_{1p}$  from eq. (5) and regarding  $k_{2p} i_2 = k_{1p} \frac{U_{12p}}{\omega L_{1p}}$  finally results in

$$B_p = \frac{\mu_0}{\delta_m} \text{Re} \left\{ k_{1p} \frac{U_1}{\omega L_1} e^{-j\varphi_{12p}} e^{-jp\theta_2} \right\}, \quad (7)$$

where it is easy to identify the complex phasor  $\underline{B}_p = \hat{B}_p e^{j\varphi_{Bp}} = \frac{\mu_0}{\delta_m} k_{1p} \frac{U_1}{\omega L_1} e^{-j\varphi_{12p}}$

### 2.3 Eccentricity Field Harmonics

The voltage equations of order  $p \pm 1$  are

$$0 = (R_{1p\pm 1} + j\omega L_{1p\pm 1}) \underline{I}_{1p\pm 1} \Rightarrow \underline{I}_{1p\pm 1} = 0 \quad (\text{stator}), \quad (8)$$

$$0 = (R_{Dp\pm 1} + js_{p\pm 1} \omega L_{Dp\pm 1}) \underline{I}_{Dp\pm 1} + \underline{U}_{21Dp\pm 1} \quad (\text{damper cage}). \quad (9)$$

Here it is assumed that the field waves of order  $p \pm 1$  cannot induce voltage into the stator phases, which is the case for integer-slot windings without parallel branches (Tüxen, 1941). The induced voltages  $\underline{U}_{21p\pm 1}$  originate from the eccentricity fields and have to be calculated subsequently. Therefore a closer look at the formation of these harmonics shall be taken here.

As it is well known, the eccentricity field harmonics arise from the multiplication of the magnetic excitation with the air gap permeance  $\Lambda(\theta) = \frac{\mu_0}{\delta(\theta)} = \frac{\mu_0}{\delta_m} \left( 1 + \frac{e}{\delta_m} \cos\theta \right) + \mathcal{O}(\varepsilon)$  (Frohne, 1968), where  $\delta(\theta)$  is the actual air gap width at a certain circumferential position  $\theta$  as shown in Fig. 2. Again, higher order terms were neglected. Multiplying with the fundamental magnetic excitation one obtains

$$\Lambda(\theta) k_{1p} \frac{U_1}{\omega L_{1p}} \cos(p\theta_2 + \varphi_{12p}) = \hat{B}_p \left( \cos(p\theta_2 - \varphi_{Bp}) + \frac{1}{2} \frac{e}{\delta_m} \cos((p \pm 1)\theta_2 + \varphi_{12p} \pm (\vartheta - \gamma)) \right), \quad (10)$$

where  $\theta = \theta_2 + (\vartheta - \gamma)$  has been inserted. In complex notation these field components read

$$\hat{B}_p \text{Re} \left\{ e^{-j(p\theta_2 + \varphi_{12p})} + \frac{1}{2} \frac{e}{\delta_m} e^{\mp j(\vartheta + \gamma)} e^{-j((p \pm 1)\theta_2 + \varphi_{12p})} \right\}. \quad (11)$$

Here it is possible to identify the phasor  $\underline{z}_2^\pm = x_2 \pm jy_2 = e e^{\mp j(\vartheta - \gamma)}$ , representing the rotor orbit position within the corotating frame of reference (compare Fig. 2). Obviously, the components of the eccentricity field harmonics shown in eq. (11) cause the mutual induced voltage in the damper cage, which is calculated by

$$u_{21Dp\pm 1} = \frac{d\Psi_{21Dp\pm 1}}{dt} = \frac{1}{2} \hat{B}_p \int_{\mathcal{M}} \frac{\partial}{\partial t} \text{Re} \left\{ \frac{\underline{z}_2^\pm}{\delta_m} e^{-j(p \pm 1)\theta_2 + \varphi_{12p}} \right\} dS, \quad (12)$$

where  $\Psi_{21Dp\pm 1}$  is the linked flux of the field components of order  $p \pm 1$ , caused by eccentricity into a representative damper mesh surface  $\mathcal{M}$ . Note that the second part of this equation refers to the moving frame of reference. Due to the fact that the damper cage mesh represents a moving surface, the Helmholtz transport theorem (see e.g. Rothwell (2008)) has to be applied. In this case the component proportional to the rotor orbital motion (motion of the damper cage surface) is of order  $\mathcal{O}(\varepsilon)$  and therefore neglected here.

Evaluating eq. (12) results in the voltage phasor

$$\underline{U}_{21Dp\pm 1} = \frac{1}{2} \hat{B}_p k_{Dp\pm 1} \frac{\dot{\underline{z}}_2^\pm}{\delta_m} e^{-j\varphi_{12p}}, \quad (13)$$

where  $k_{Dp\pm 1}$  is a constant similar to  $k_{1p}$  and  $k_{2p}$ , depending on the machine geometry and damper cage design. At this point a major drawback modelling the electrical voltages and currents as pure AC quantities shall be pointed out: considering eq. (13) it is found that the voltage phasor depends on the time derivative of the rotor orbital

motion  $\dot{z}_2^\pm$ . This result contradicts the model assumption of a harmonic time dependency and would only be permissible, if the time rate of change of  $\dot{z}_2^\pm$  would be small compared to the frequency of  $u_{21Dp\pm 1}$ , what might not be the case.

Nethertheless, inserting the result into the damper cage voltage equation (9) and solving for the current phasors  $\underline{I}_{Dp\pm 1}$  yields

$$\underline{I}_{Dp\pm 1} = -\frac{j s_{p\pm 1}}{\beta + j s_{p\pm 1}} \frac{U_{21Dp\pm 1}}{j s_{p\pm 1} \omega L_{Dp\pm 1}}. \quad (14)$$

Here the resistance to reactance ratio  $\beta = \frac{R_{Dp\pm 1}}{\omega L_{Dp\pm 1}}$  for the damper cage has been introduced as it is usually done in literature (Früchtenicht (1982), Jordan (1969)) and the complex number  $-\frac{j s_{p\pm 1}}{\beta + j s_{p\pm 1}} = (a_{p\pm 1} - 1) + j b_{p\pm 1}$  is identified as the complex field damping factor.

Finally, the field component of the eccentricity harmonics, caused by the damper cage reads

$$\frac{\mu_0}{\delta_m} \text{Re} \left\{ k_{Dp\pm 1} \underline{I}_{Dp\pm 1} e^{-j(p\pm 1)\theta_2} \right\} = -\frac{1}{2} \hat{B}_p \text{Re} \left\{ \frac{1}{\beta + j s_{p\pm 1}} \frac{1}{\omega \delta_m} \dot{z}_2^\pm e^{-j((p\pm 1)\theta_2 + \varphi_{12p})} \right\}. \quad (15)$$

Adding this result to the eccentricity harmonics, caused by the air gap permeance (eq. (11)) results in

$$B_{p\pm 1} = \frac{1}{2} \hat{B}_p \text{Re} \left\{ \left( \frac{\dot{z}_2^\pm}{\delta_m} - \frac{1}{\beta + j s_{p\pm 1}} \frac{1}{\omega \delta_m} \dot{z}_2^\pm \right) e^{-j\varphi_{12p}} e^{-j(p\pm 1)\theta_2} \right\}. \quad (16)$$

With this result also the complex amplitudes  $\underline{B}_{p\pm 1} = \hat{B}_{p\pm 1} e^{j\varphi_{Bp\pm 1}} = \frac{1}{2} \hat{B}_p \left( \frac{\dot{z}_2^\pm}{\delta_m} - \frac{1}{\beta + j s_{p\pm 1}} \frac{1}{\omega \delta_m} \dot{z}_2^\pm \right) e^{-j\varphi_{12p}}$  are known.

Considering eq. (1) for the magnetic field only  $B_0$  is left undetermined until now. As mentioned before it results in a homopolar flux in 2-pole machines and can be calculated as proposed by Belmans (1987). Assuming maximum homopolar flux leading to maximum electromagnetic forces, a worst case scenario considering rotordynamics will be investigated in this work. This assumption leads to  $B_0 = 0$  completing the derivation of the magnetic field formula.

## 2.4 Electromagnetic Forces

The electromagnetic forces can be calculated using the Maxwell stress tensor (Rothwell, 2008). For the sake of simplicity, stress is integrated over the stator surface here. As higher order terms have been neglected (resulting in a straight radial flux density) the force formula reads

$$\vec{F}_2 = -\vec{F}_1 = F_{x_2} \vec{e}_{x_2} + F_{y_2} \vec{e}_{y_2} = \frac{1}{2\mu_0} \int_{\partial\Omega_1} B^2 \vec{e}_r dS. \quad (17)$$

The calculation will be carried out in the rotor fixed frame of reference, where  $\vec{e}_r = \cos \theta_2 \vec{e}_{x_2} + \sin \theta_2 \vec{e}_{y_2}$  and  $dS = r_1 \ell d\theta_2$  with the effective length  $\ell$  of the air gap.

Calculating the force components  $F_{x_2}$  and  $F_{y_2}$  involves some algebra and has to be done individually for the cases  $p > 1$  (machines with more than two poles) and  $p = 1$  (2-pole machines). As it is usual in rotordynamics (Gasch, 2006), matrix notation will be used further on. In this context, a matrix  $\underline{M}$  is displayed in bolt letters.

In the first case ( $p > 1$ ) one finds

$$\begin{bmatrix} F_{x_2} \\ F_{y_2} \end{bmatrix} = \begin{bmatrix} \text{Re} \{ \underline{B}_p \overline{\underline{B}_{p\pm 1}} \} \\ \text{Im} \{ \mp \underline{B}_p \overline{\underline{B}_{p\pm 1}} \} \end{bmatrix} \quad \text{and} \quad \begin{bmatrix} F_{x_2} \\ F_{y_2} \end{bmatrix} = \begin{bmatrix} \text{Re} \{ \underline{B}_p \overline{\underline{B}_{p\pm 1}} + \underline{B}_p \overline{\underline{B}_{p-1}} \} \\ \text{Im} \{ \mp \underline{B}_p \overline{\underline{B}_{p\pm 1}} + \underline{B}_p \overline{\underline{B}_{p-1}} \} \end{bmatrix} \quad (18)$$

in the second case ( $p = 1$ ). Here, the field wave of order  $\nu = p - 1 = 0$  is homopolar, creating additional force components. Note that the value of  $p$  for  $p = 1$  is not inserted for the sake of comparability here and in the following considerations.

Evaluating the expressions in eqs. (18) respectively yields

$$\begin{bmatrix} F_{x_2} \\ F_{y_2} \end{bmatrix} = \underbrace{c_{elm} \mathbf{I}}_{\mathbf{F}_{UMP}} \begin{bmatrix} x_2 \\ y_2 \end{bmatrix} - \underbrace{\frac{c_{elm}}{\omega} \mathbf{P}_1}_{\mathbf{F}_{FD}} \begin{bmatrix} \dot{x}_2 \\ \dot{y}_2 \end{bmatrix}, \quad (19)$$

in the first case ( $p > 1$ ), where FD stands for field damping and where  $\mathbf{I}$  is the identity matrix and

$$\mathbf{P}_1 = \frac{1}{2} \begin{bmatrix} \frac{\beta}{\beta^2 + s_{p+1}^2} + \frac{\beta}{\beta^2 + s_{p-1}^2} & \left( \frac{s_{p+1}}{\beta^2 + s_{p+1}^2} - \frac{s_{p-1}}{\beta^2 + s_{p-1}^2} \right) \\ - \left( \frac{s_{p+1}}{\beta^2 + s_{p+1}^2} - \frac{s_{p-1}}{\beta^2 + s_{p-1}^2} \right) & \frac{\beta}{\beta^2 + s_{p+1}^2} + \frac{\beta}{\beta^2 + s_{p-1}^2} \end{bmatrix}. \quad (20)$$

In the second case ( $p = 1$ ) the result is

$$\begin{bmatrix} F_{x_2} \\ F_{y_2} \end{bmatrix} = \underbrace{c_{elm} (\mathbf{I} + \mathbf{T})}_{\mathbf{F}_{UMP}} \begin{bmatrix} x_2 \\ y_2 \end{bmatrix} - \underbrace{\frac{c_{elm}}{\omega} (\mathbf{P}_1 + \mathbf{P}_2 \mathbf{T})}_{\mathbf{F}_{FD}} \begin{bmatrix} \dot{x}_2 \\ \dot{y}_2 \end{bmatrix} \quad (21)$$

with

$$\mathbf{T} = \frac{1}{2} \begin{bmatrix} \cos(2\varphi_{12p}) & -\sin(2\varphi_{12p}) \\ -\sin(2\varphi_{12p}) & -\cos(2\varphi_{12p}) \end{bmatrix} \quad \text{and} \quad \mathbf{P}_2 = \begin{bmatrix} \frac{\beta}{\beta^2 + s_{p-1}^2} & \frac{s_{p-1}}{\beta^2 + s_{p-1}^2} \\ -\frac{s_{p-1}}{\beta^2 + s_{p-1}^2} & \frac{\beta}{\beta^2 + s_{p-1}^2} \end{bmatrix}. \quad (22)$$

The electromagnetic spring constant in eqs. (19) and (21) is  $c_{elm} = \frac{\pi r_1 \ell \hat{B}_p^2}{2\mu_0 \delta_m}$ . There are additional forces proportional to the rotor orbit velocity, which had not been considered in earlier works: these forces originate from field damping. As they are due to induction and as the voltage equations have been solved for the induced currents explicitly the forces usually proportional to the currents are now proportional to the rotor orbit velocity.

Components on the main diagonal can be considered as inner damping (compare Gasch (2006)), as the coefficients in  $\mathbf{P}_1$  and  $\mathbf{P}_2$  are positive. Components at the secondary diagonal correspond to gyroscopic effects relative to the moving frame of reference. As it is well known from classical rotordynamics, inner damping is a typical source of self-excited oscillations and in fact it is the only possible source here.

## 2.5 Rotor Model

The mechanical system is modelled as a classical Laval-rotor (Jeffcott-rotor). With this model one mode shape of the generator system can be depicted and analysed dynamically. The basic assumptions are that the rotor consists of a massless elastic shaft (isotropic stiffness  $c$ ) supported by isotropic rigid bearings with a circular rigid disk on it. The centre of inertia  $S$  shall be eccentric causing imbalance. Combined with the forces of electromagnetic origin the equations of motion read

$$\begin{bmatrix} m & 0 \\ 0 & m \end{bmatrix} \begin{bmatrix} \ddot{x}_2 \\ \ddot{y}_2 \end{bmatrix} + \begin{bmatrix} d + d_i & -2m\Omega \\ 2m\Omega & d + d_i \end{bmatrix} \begin{bmatrix} \dot{x}_2 \\ \dot{y}_2 \end{bmatrix} + \begin{bmatrix} c_x - m\Omega^2 & -d\Omega \\ d\Omega & c_y - m\Omega^2 \end{bmatrix} \begin{bmatrix} x_2 \\ y_2 \end{bmatrix} = m\Omega^2 \begin{bmatrix} e_{Sx} \\ e_{Sy} \end{bmatrix} + \begin{bmatrix} F_{x_2} \\ F_{y_2} \end{bmatrix} \quad (23)$$

in the rotor fixed corotating frame of reference. Here  $\Omega = \frac{\omega}{p}$  is the synchronous angular velocity of the rotor and  $m$  is the rotor mass. In eq. (23) two different kinds of mechanical damping are introduced: one damping force  $\mathbf{F}_D = -d\dot{\mathbf{x}}_1$ , proportional to the inertial orbital velocity  $\mathbf{x}_1$  of the rotor and another force  $F_{D_i} = -d_i \dot{\mathbf{x}}_2$ , proportional to the orbital velocity  $\dot{\mathbf{x}}_2$  of the rotor relative to the corotating frame of reference. While the first damping force accounts for air friction etc., the second one is due to internal friction, e.g. at joints on the rotor. The mechanical spring constants  $c_x$  (along a certain pole axis) and  $c_y$  (perpendicular to that) are equal in machines with more than two poles ( $c_x = c_y$  if  $p > 1$ ) and different in machines with two poles ( $c_x \neq c_y$  if  $p = 1$ ), due to the rotor construction (Gasch, 2006). The values  $(e_{Sx}, e_{Sy}) = \text{const.}$  are the positional coordinates of the centre of inertia in the rotor fixed frame of reference.

In the following the parameters and variables

$$\omega_0 = \sqrt{\frac{c}{m}}, \quad \tau = \omega_0 t, \quad \eta = \frac{\Omega}{\omega_0} = \frac{\omega}{p\omega_0}, \quad D = \frac{d}{2m\omega_0},$$

$$D_i = \frac{d_i}{2m\omega_0}, \quad c = \frac{c_x + c_y}{2}, \quad \kappa = \frac{c_x - c_y}{c_x + c_y}, \quad \zeta = \frac{c_{elm}}{c},$$

are introduced. In this context  $\omega_0$  is the angular eigenfrequency of the corresponding undamped system without electromagnetic forces,  $\tau$  is a dimensionless timescale,  $D$  and  $D_i$  are mechanical damping ratios,  $c$  is the mean spring constant and  $\kappa$  is a measure for the noncircularity of the rotor shaft. This parameter is  $\kappa = 0$  for machines with more than two poles ( $p > 1$ ), and  $\kappa \neq 0$  for 2-pole machines ( $p = 1$ ). The parameters  $\eta$  and  $\zeta$  will be explained below. Using these definitions eqs. (23) transform to

$$\begin{bmatrix} x_2'' \\ y_2'' \end{bmatrix} + \begin{bmatrix} 2(D + D_i) & -2\eta \\ 2\eta & 2(D + D_i) \end{bmatrix} \begin{bmatrix} x_2' \\ y_2' \end{bmatrix} + \begin{bmatrix} 1 + \kappa - \eta^2 & -2D\eta \\ 2D\eta & 1 - \kappa - \eta^2 \end{bmatrix} \begin{bmatrix} x_2 \\ y_2 \end{bmatrix} - \frac{\zeta}{c_{elm}} \begin{bmatrix} F_{x_2} \\ F_{y_2} \end{bmatrix} = \eta^2 \begin{bmatrix} e_{Sx} \\ e_{Sy} \end{bmatrix} \quad (24)$$

where  $(\prime)$  indicates the derivative with respect to the nondimensional time  $\tau$ . The factor  $\zeta = \frac{c_{elm}}{c}$  represents the relative strength of the electromagnetic forces, which are dependent on the electromagnetic machine design. Its order of magnitude is usually below 10%. Additionally the term  $\frac{1}{\omega}$  in eqs. (19) and (21) becomes  $\frac{1}{p\eta} = \frac{\omega_0}{\omega}$ . Here  $\eta$  is the mechanical speed of rotation compared to the critical speed of the system. Usually machines running far below this critical speed ( $\eta = 1$ ) are denoted as rigid shaft machines, while the ones running above it are known as soft mounted (Dawson, 1983).

### 3 Results

Eq. (24) is an inhomogenous system of two ODEs of second order with constant coefficients for the orbital motion  $\mathbf{q} = [x_2 \ y_2]^T$  of the rotor. Its solution is described by a homogenous- and an inhomogenous part ( $\mathbf{q}_h$  and  $\mathbf{q}_p$ ). The latter one represents the steady state solution, when free oscillations have vanished. In view of electromagnetically excited oscillations especially the question of self-excited oscillations is of great interest (Früchtenicht, 1982). Therefore in this section a stability analysis will be carried out posing the question under which circumstances free oscillations (homogenous solution) of exponentially rising amplitude may occur. Therefore an ansatz of the kind  $\mathbf{q}_h = \mathbf{q} - \mathbf{q}_p = \mathbf{r}e^{\lambda\tau}$ , where  $\lambda$  is an eigenvalue and  $\mathbf{r}$  is a corresponding eigenvector, is made and the characteristic polynomial in  $\lambda$  is derived. Applying Hurwitz' criterion (see e.g. Merkin (2012)) inequalities for the stability of the steady state can be found. These expressions describe regions in the parameter space where free oscillations decay (stable steady state) or rise (unstable steady state).

Before presenting stability maps a short view on relevant system parameters shall be given: Besides the mechanical parameters  $\eta$ ,  $\kappa$  and  $D$  and  $D_i$ , there are three electromagnetic parameters:  $\zeta$ ,  $\varphi_{12p}$  and  $\beta$ . The parameter  $\zeta$  for the relative strength of the electromagnetic forces has already been explained. As it turns out in the following, its influence on the stability is quite significant. Furthermore the electrical torque angle  $\varphi_{12p}$  and the resistance to reactance ratio  $\beta$  play a role in this context. For generators the torque angle is in between  $\varphi_{12p} = 0$  (no load) and  $\varphi_{12p} = \frac{\pi}{2}$  (critical load). Despite that it will not exceed  $\frac{\pi}{4}$  under normal load conditions. The resistance to reactance ratio  $\beta$  has an order of magnitude of  $\mathcal{O}(10^{-1})$ . As the influence of the mechanical parameters  $D$  and  $\kappa$  is known, their values are set to  $D = 0.002$  (weak damping) and  $\kappa = 0.1$  in the case of 2-pole machines. The influence of all other parameters will be shown subsequently.

Fig. 3 shows two basic stability maps plotting the regions of stable and unstable states in the parameter space. In the figure the force parameter  $\zeta$  is plotted against the specific rotational speed  $\eta$  for a 4-pole machine (Fig.3 (a)) and a 2-pole machine (Fig.3 (b)) considering homopolar fluxes, respectively. Each map shows stable regions in white and unstable states in grey for a basic parameter configuration. Note that changing the specific rotational speed  $\eta = \frac{\Omega}{\omega_0}$  does not mean changing to the absolute running speed of the machine, which is fix and given by  $\Omega = \frac{\omega}{p}$ , but changing the critical speed  $\omega_0$  relative to  $\Omega$ . Thus in Fig. 3 different machine designs are compared.

Analysing the stability behaviour different aspects raise the attention: As a first point both maps show an unstable region at high rotational speeds and high electromagnetic forces. In both cases one finds, that the higher the nominal rotational speed compared to the critical speed, the more likely it seems to be, that a stable state becomes unstable. As a major difference, 2-pole machines (Fig. 3 (b)) have two additional regions of unstable states. One narrow region around the critical speed ( $\eta = 1$ ), which corresponds to the one found in earlier works (Kellenberger (1966), Boy (2015)) and one at very low running speeds and low values of  $\zeta$ . The region around  $\eta = 1$  originates

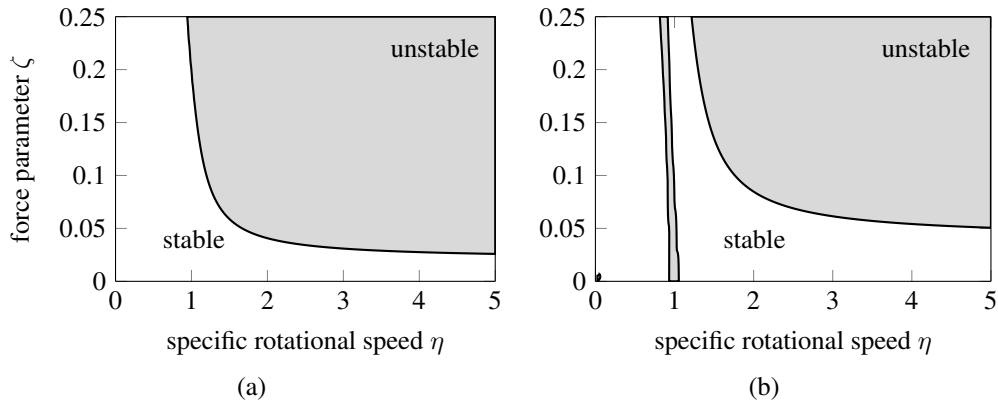


Figure 3. Stability map for the steady state of a 4-pole (a) and a 2-pole machine (b). Here  $D = 0.002$ ,  $D_i = 0$ ,  $\varphi_{12p} = \frac{\pi}{8}$  and  $\beta = 0.1$  were chosen.

from the shaft noncircularity. Fig. 3 (b) shows that it is affected by the electromagnetic forces, as the critical speed is reduced with higher values of  $\zeta$ . The second additional region is very small and seems not to be relevant for normal operational conditions. It originates from homopolar fluxes.

As stated before additional forces due to field damping can be compared to inner mechanical damping. To analyse their effect, consider Fig. 4, which shows a classical stability map considering the influence of inner mechanical damping for the example of a 4-pole machine. Here the damping ratio  $\frac{D}{D_i}$  is plotted against the specific rotational speed  $\eta$ . From literature (Gasch, 2006) it is known, that in presence of inner damping, a certain critical speed depending on the damping ratio exists. Introducing electromagnetic forces to the system changes this map significantly, as indicated by dashed lines in the map. These lines show the stability border, if the resistance to reactance ratio  $\beta$  is increased from 0 by 0.025 to 0.1. Here it becomes obvious, that field damping may reduce the stability of the steady state. However, it should be noted here that the shown effect becomes weaker, if the mechanical damping forces become stronger compared to the electromagnetic forces.

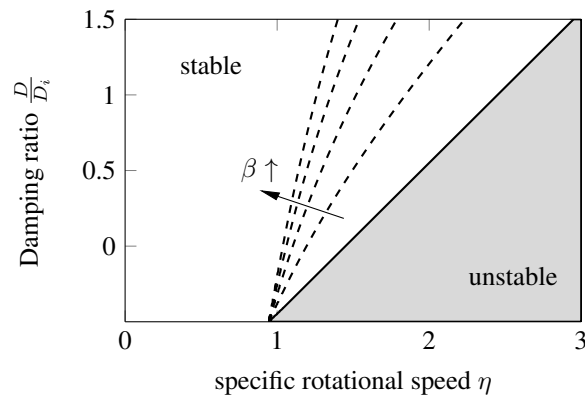


Figure 4. Stability map for the steady state of a 4-pole machine comparing the mechanical and inner Damping varying  $\beta$  from 0 by 0.025 to 0.1. All remaining parameters are chosen according to Fig. 3.

Having discussed the basic stability behaviour, a short view on parameter influence shall be taken as a last point of this section. For the sake of brevity these results are not shown explicitly, but simply explained.

Rising the number of pole pairs moves the stability border (critical speed in Fig. 3) towards lower values of  $\eta$ . This fact shows that self-excited oscillations become more likely in machines with a higher number of pole pairs. Although this model is not well suited for non-salient pole generators (which have even more magnetic poles), they might be even more sensitive to such oscillations.

Considering the stability conditions derived from Hurwitz' criterion one finds that the load condition (torque angle  $\varphi_{12p}$ ) does not affect generators with more than two magnetic poles. However, in 2-pole machines when homopolar fluxes are present the picture changes. While in this case the narrow region of unstable states around  $\eta = 1$  (Fig.3 (b)) grows with increasing torque angle, the border of critical speeds for the region caused by field damping is slightly shifted towards higher rotational speeds. Furthermore the small region at very low speeds becomes larger.

## 4 Summary and Conclusions

Within this contribution the effect of field damping on lateral rotordynamics of non-salient pole generators has been investigated. The implemented electro-mechanical model comprises the electrical circuits of the stator and the rotor, as well as a damper cage, an approximation to the involved magnetic field problem and a Laval-rotor (Jeffcott-rotor). It has been shown that the currents flowing in the damper cage are affected by the orbital motion of the rotor and that there is a back coupling via electromagnetic forces exerted by the magnetic field. The mathematical structure of these forces is similar to inner mechanical damping and depends on the rotational speed of the machine, the machine design in general and the electrical properties of the damper cage. The survey has clarified that self-excited oscillations might occur in machines operating under high nominal rotational speeds compared to their critical speed. The stability behaviour is different for 2-pole machines and ones with a higher number of pole pairs due to the occurring homopolar fluxes in the first case.

In future surveys it would be sensible to reconsider the modelling in detail. At the one hand side, a major model contradiction concerning the assumptions of AC voltages in the damper cage has been found and at the other hand side effects like saturation should not be neglected. As a further point the model should be validated by more detailed numerical simulations and practical experiments.

Recently the authors pointed out, that rotational disturbances (e.g. hunting) may also significantly influence the steady state stability (Boy, 2016). A combined investigation of field damping and these effects could also be considered.

## References

- [1] Arkkio, A. et al. (2000): Electromagnetic force on a whirling cage rotor. IEE Proceedings-Electric Power Applications, **147**, pp. 353–360.
- [2] Belmans, R. and Vandenput, A. and Geysen, W. (1987): Calculation of the flux density and the unbalanced pull in 2-pole induction machines. Electr. Eng. (Archiv für Elektrotechnik), **70**, pp. 151–161.
- [3] Boy, F. and Hetzler, H. (2015): Rotordynamics of two-pole turbogenerators with refined modelling of the unbalanced magnetic pull. Proc. Appl. Math. Mech., **15**, pp. 243–244.
- [4] Boy, F. and Hetzler, H., Ph. Schäfer (2016): On the rotordynamical stability of synchronous electric machinery considering different load cases and operating conditions. Proc. ISMA 2016, pp. 837–849.
- [5] Burakov, A. and Arkkio, A. (2006): Low-order parametric force model for eccentric-rotor electrical machine with parallel connections in stator winding. IEE Proceedings-Electric Power Applications, IET, **153**, pp. 592–600.
- [6] Dawson, R. and Eis, R. (1983): Specifying and designing flexible shaft electrical machines. IEEE transactions on industry applications, **6**, pp. 985–995.
- [7] Dorrell, D.-G. et al. (2011): Damper windings in induction machines for reduction of unbalanced magnetic pull and bearing wear. 2011 IEEE Energy Conversion Congress and Exposition, **49**, pp. 1612–1619.
- [8] Frohne, H. (1968): Über den einseitigen magnetischen Zug in Drehfeldmaschinen. Electr. Eng. (Archiv für Elektrotechnik), **51**, pp. 300–308.
- [9] Früchtenicht, J. (1982): Exzentrizitätsfelder als Ursache von Laufinstabilitäten bei Asynchronmaschinen. Electr. Eng. (Archiv für Elektrotechnik), **65**, pp. 271–281.
- [10] Gasch, R. and Nordmann, R. and Prützner H. (2006): *Rotordynamik*. Springer-Verlag, Berlin Heidelberg.
- [11] Jordan, H. and Weis, M. (1970): *Synchronmaschinen I*. Vieweg & Sohn, Braunschweig.
- [12] Jordan, H. and Weis, M. (1969): *Asynchronmaschinen*. Springer Fachmedien, Wiesbaden.
- [13] Kaehne, P. (1963): Unbalanced Magnetic Pull in Rotating Electric Machines: Survey of Published Work. ERA Report, **142**.
- [14] Kellenberger, W. (1966): Der magnetische Zug in Turbogenerator-Rotoren als Ursache einer Instabilität des mechanischen Laufes. Electr. Eng. (Archiv für Elektrotechnik), **50**, pp. 253–265.
- [15] Merkin, D. (2012): *Introduction to the Theory of Stability*. Springer Science & Business Media, New York.

- [16] Rothwell, E.-J. and Michael J.-C. (2008): *Electromagnetics*. CRC press, Boca Raton.
- [17] Tüxen, E. (1941): Das Oberwellenverhalten mehrphasiger Wechselstromwicklungen. Jahrbuch d. AEG-Forschung, **78**.
- [18] Wallin, M. and Bladh, J. and Lundind, U. (2013): Damper winding influence on unbalanced magnetic pull in salient pole generators with rotor eccentricity. IEEE Transactions on Magnetics, **49**, pp. 5158–5165.

## Nomenclature

$r_1$	stator radius	$a_1$	current sheet stator
$r_2$	rotor radius	$a_2$	current sheet rotor
$\mathcal{K}$	cartesian coordinate system	$N_D$	number of damper cage bars
$\mathcal{Z}$	cylindrical coordinate system	$\varphi_k$	electrical phase angle
$\vec{e}_x, \vec{e}_y, \vec{e}_z$	cartesian basis vectors	$p$	number of pole pairs
$\vec{e}_r, \vec{e}_\theta, \vec{e}_z$	cylindrical basis vectors	$\nu$	number of field harmonic
$r, \theta, z$	cylindrical coordinates	$\varepsilon = \frac{\delta_m}{r_2}$	small parameter
$e$	rotor eccentricity	$B$	magnetic flux density
$\gamma$	rotor eccentricity phase angle	$j$	imaginary unit
$\vartheta$	rotor angle	$\underline{A}$	complex quantity
$\delta(\theta)$	actual air gap width at angle $\theta$	$\overline{A}$	complex conjugate
$\Omega$	air gap region	$u(t)$	voltage
$\partial\Omega$	air gap region boundary	$\underline{U}$	voltage phasor (particular solution)
$\mathcal{M}$	representative damper cage mesh	$i(t)$	current
$\mu_0$	magnetic field constant	$\underline{I}$	current phasor (particular solution)
$k$	machine winding parameter	$\omega_\nu$	angular frequency of $\nu$ -th harmonic
$\Lambda(\theta)$	air gap permeance at angle $\theta$	$s_\nu$	slip of $\nu$ -th harmonic
$\underline{z}^\pm$	rotor eccentricity phasor	$\omega$	supply angular frequency
$\Psi$	flux linkage	$R$	resistance
$\vec{F}_1$	force acting on the stator	$L$	inductivity
$\vec{F}_2$	force acting on the rotor	$\beta$	specific resistance of damper cage
$\ell$	effective air gap length	$S$	center of inertia
$\mathbf{I}$	unity matrix	$\frac{\omega}{p}$	synchronous angular frequency
$\mathbf{P}_1, \mathbf{P}_2$	force matrix damper cage	$\omega_0$	angular eigenfreq. (undamped system)
$\mathbf{T}$	transformation matrix (homopolar flux)	$\eta$	specific rotor speed
$c_{elm}$	electromagnetic stiffness constant	$\kappa$	noncircularity parameter
$c$	mechanical stiffness constant	$\zeta$	specific electromagnetic stiffness
$c_x$	mechanical stiffness constant (x-direction)	$\tau$	nondimensional time
$c_x$	mechanical stiffness constant (y-direction)	$(\ )'$	nondimensional time derivative
$m$	rotor mass	$\mathbf{q}$	mechanical position matrix
$d$	external damping constant	$\mathbf{q}_h$	homogenous solution
$D$	specific external damping constant	$\mathbf{q}_p$	particular solution
$d_i$	internal damping constant	$\lambda$	eigenvalue
$D_i$	specific internal damping constant	$\mathbf{r}$	eigenvector